Calibrating M-Sequence GPTSs with uncertainty quantification and cyclostratigraphy

Jordan Hildebrandt (Wittenberg) – Dr. Alberto Malinverno, advisor, LDEO

Supported by NSF OCE 09-26306

Introduction

Geomagnetic polarity timescales (GPTSs) are vital to date events in the geological record. GPTSs are based on "block models" of magnetic anomaly lineations measured on the flanks of mid-ocean ridges. Current GPTSs of the Mesozoic M-sequence lineations are based on unrealistic, constant-spreading-rate assumptions, do not use all available block models, do not incorporate cyclostratigraphic constraints, and lack stringent uncertainty tabulations. This project will do all these things by limiting the variation in spreading rates for ALL magnetic anomaly block models. Doing so will result in an improved GPTS.

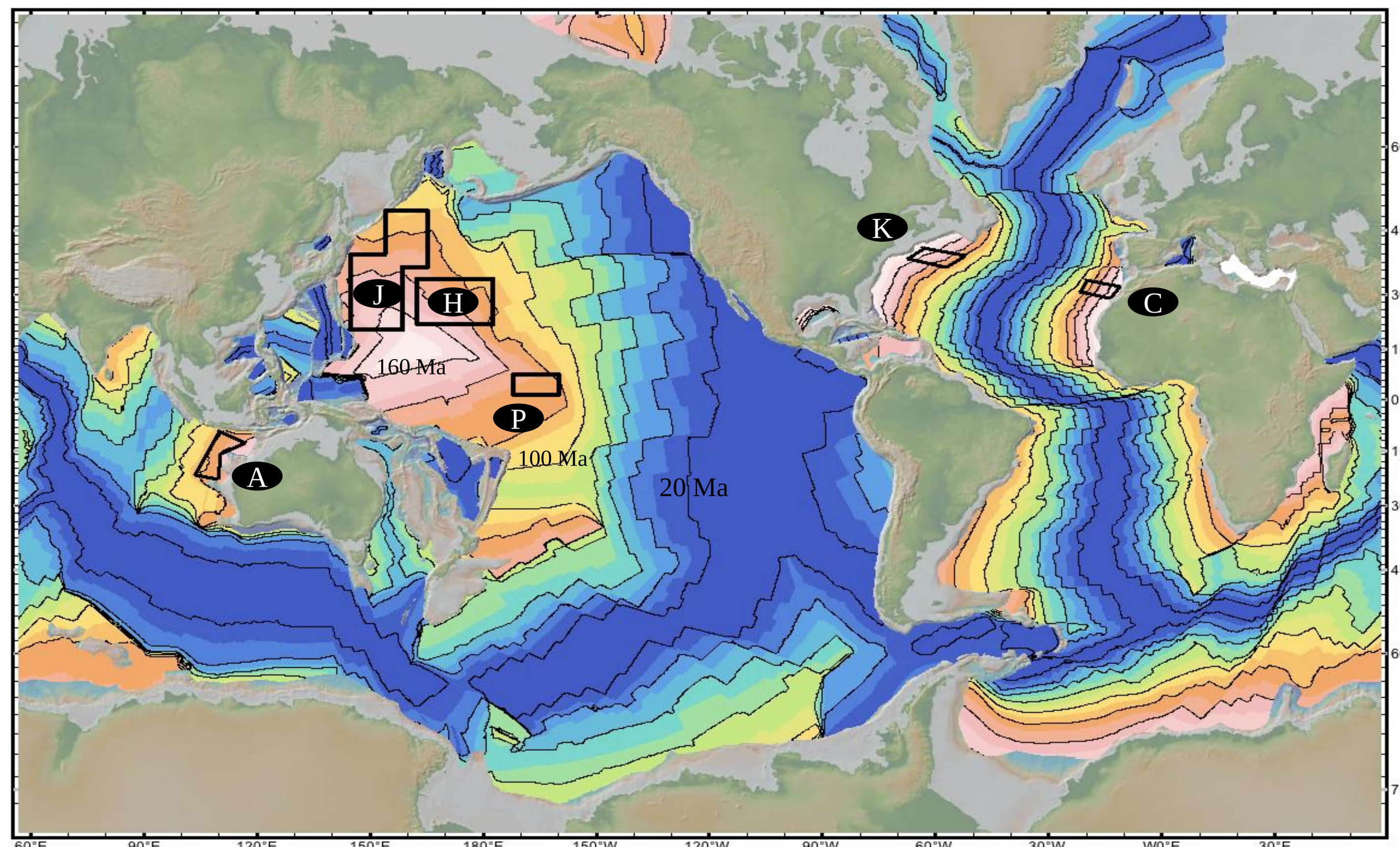

Fig. 1: Map of the age of the ocean floor and the location of the block model profiles (20 Ma contours)

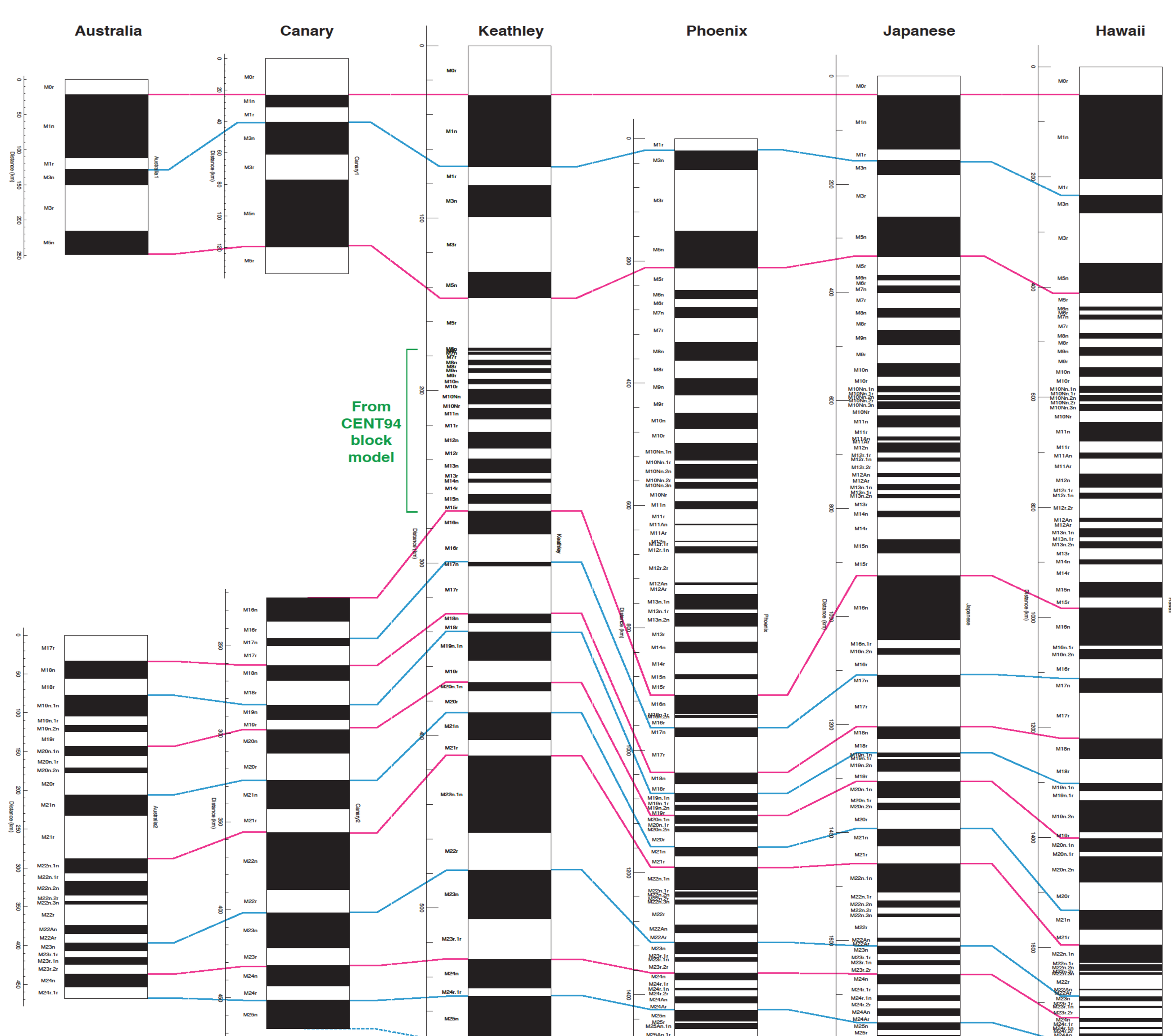

Fig. 2: Comparison chart of magnetic anomaly block models for all available profiles. Each period is called a "chron," and periods of "normal"/current polarity are black. (Tominaga and Sager, 2010, for all except where marked from CENT94 (Channell, et al., 1994))

Method

We construct the timescale by using the Metropolis algorithm, described in Chib and Greenberg, 1995, in the context of MatLab coding and a Monte Carlo sampling method. First, a candidate GPTS is generated by altering a chron duration slightly and stretching the timescale to fit radiometric age constraints. Then, its likelihood of being a good fit is calculated. The likelihood is high when the spreading rate variations implied by the timescale are small and when the durations prescribed by cyclostratigraphy are matched. If the candidate is accepted, it becomes the next step in a random walk that explores the space of possible GPTSs (see Fig. 3). The resulting sample of GPTSs is saved, and the mean GPTS and its variance are derived from this array of sampled values, which span the range of likely GPTSs.

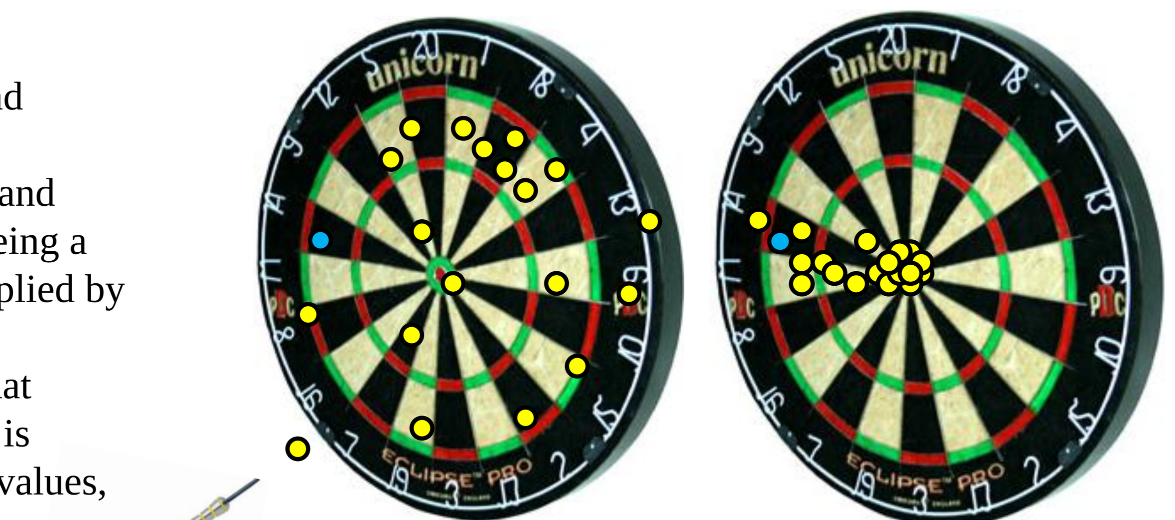

Fig. 3: Instead of an inefficient, random sample (left board), we generate new GPTSs from a random walk (right board). Each successive sample is a small step away from the previous sample. This method quickly reaches the target center after a brief "burn-in period," but it also explores the area around it, generating an uncertainty measurement (see Fig. 5 below).

Data Constraints

1. Methodology to minimize spreading rate variation

2. Absolute Ages
(Gradstein, et al., 2004; Tominaga and Sager, 2010).

Chron	Age (Ma)	St. Dev.
Base of M0r	125.0	0.5
Base of M26r	155.7	3.4

3. Durations from cyclostratigraphy
(Malinverno, et al, 2010 for M0; Fiet and Goran, 2000, for the rest)

Chron	Age (Ma)	St. Dev.
M0r	0.49	0.05
M1n	2.28	0.24
M1r	0.43	0.21
M3n	0.7	0.19
M3r	1.75	0.24

Results

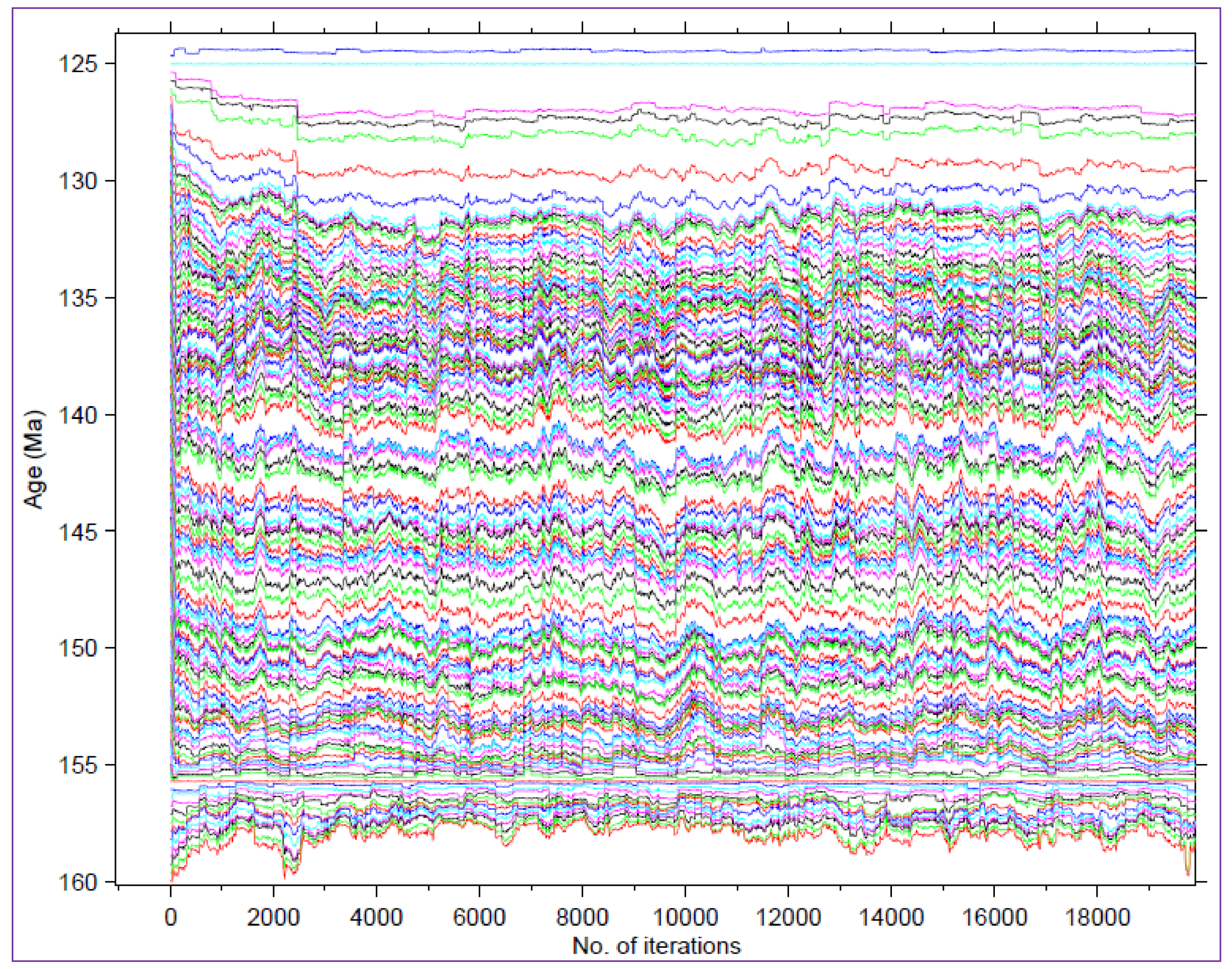

Fig. 4: (At left) shows the evolution of the GPTS, starting with equivalent chron lengths. The absolute ages have been fixed in this plot for clarity, and only the first 20,000 (out of 1 million) iterations are shown.

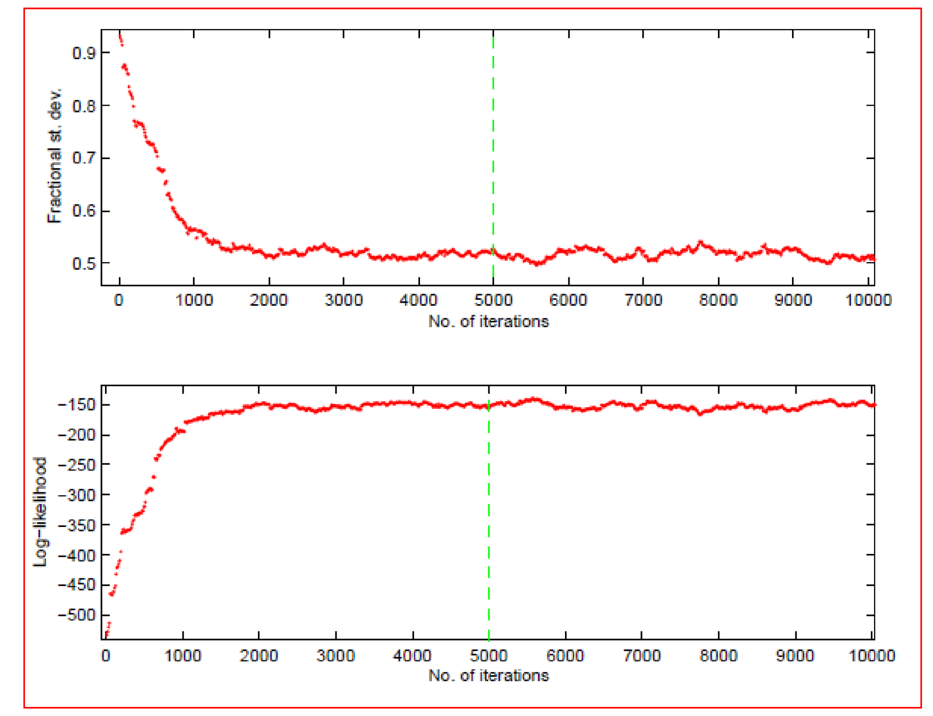

Fig. 5: (Above) also shows how quickly the Metropolis algorithm 'figures things out' – this time in terms of the log-likelihood and the fractional standard deviation.

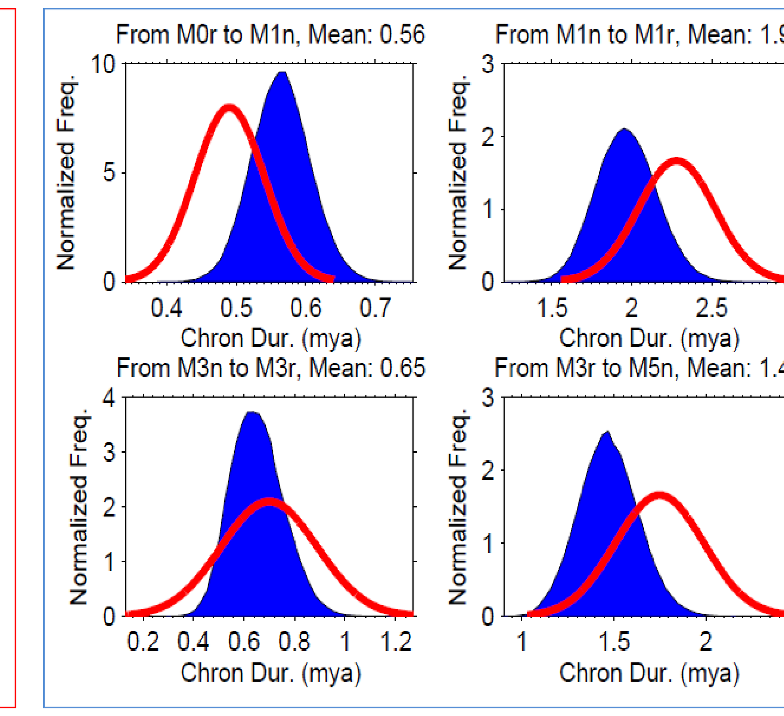

Fig. 6: (At left) Histograms of the sampled durations for each cyclostratigraphy chron compared to the input constraint (red curve).

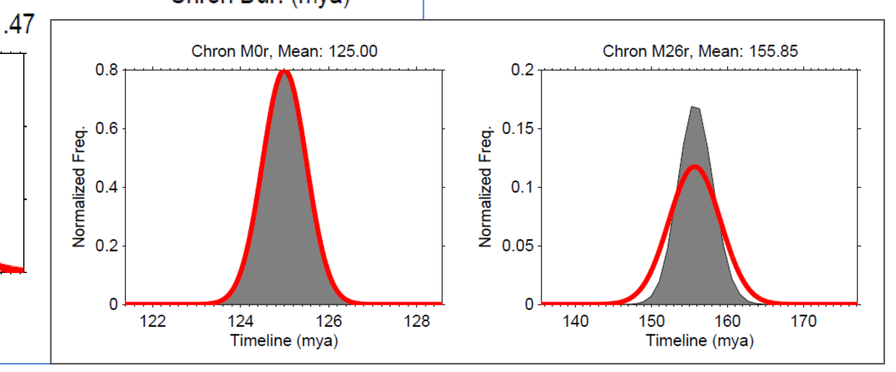

Fig. 7: (Below) Histograms of the sampled ages for each radiometric age compared to the input constraint (red curve).

Fig. 8-10: (Below) The final timescale and its associated boundary and duration standard deviations, respectively. The green lines indicate where the absolute age dates fall. The top of M0r is at 124.4 +/- .5 Ma, and the bottom of M29r is 158.1 +/- 2.5 Ma.

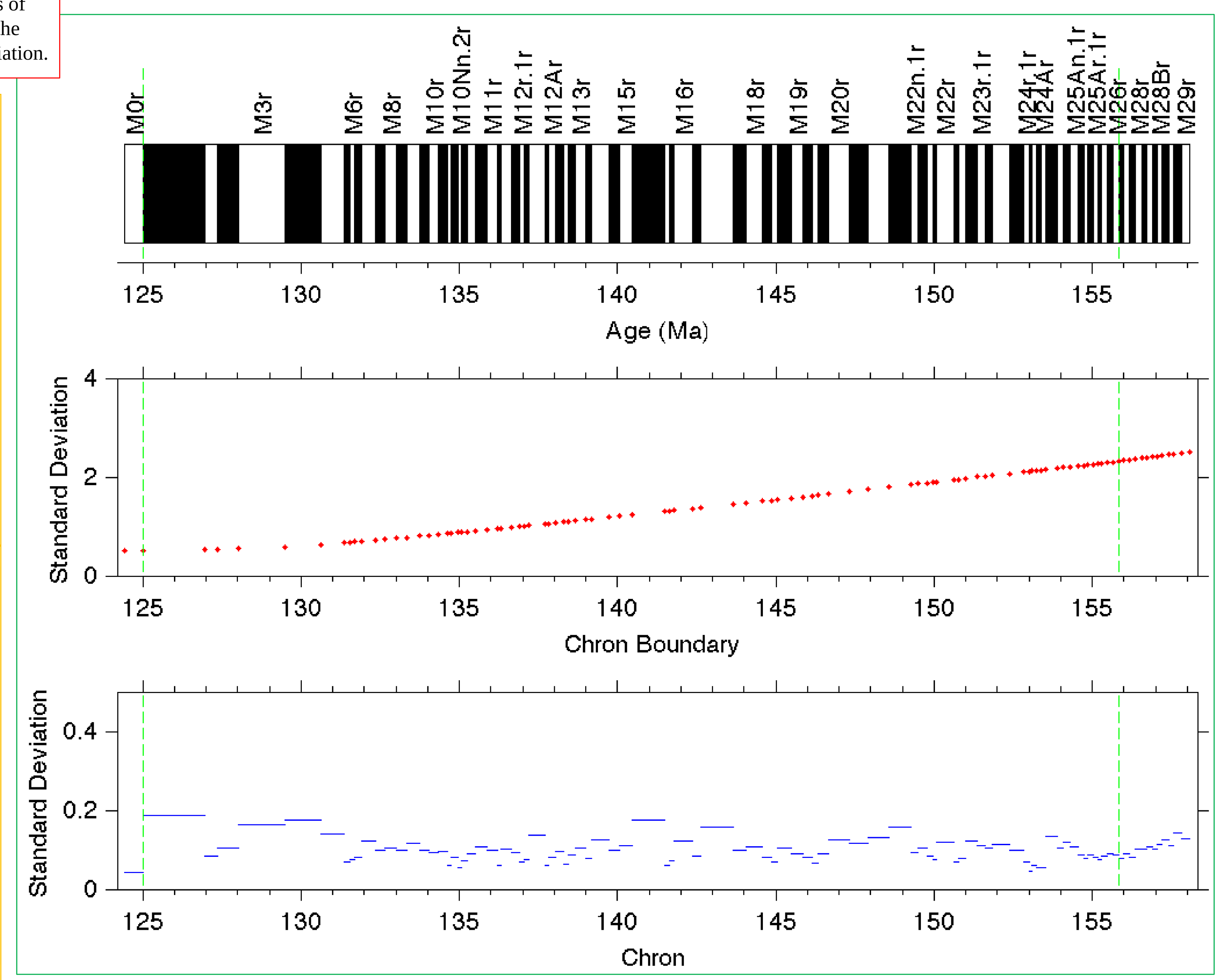

Comparison of timescales

The plots show an improvement between the TS2010 timescale (Tominaga and Sager, 2010; Fig. 11) and a random walk down the streets of the Metropolis (Fig. 12). The overall variation in spreading rates decreases from 50.9% to 43.7%. At the price of a small increase in the spreading rate variability in the Japanese and Hawaiian block models (red ovals in Fig. 12), spreading rates are less variable in all the other block models (green ovals in Fig. 12). The GPTS we constructed uses all block models, whereas TS2010 only considered the Pacific block models and also did not account for cyclostratigraphy constraints. Our method systematically accounts for uncertainties in the GPTS and can immediately produce an updated GPTS with new data/constraints.

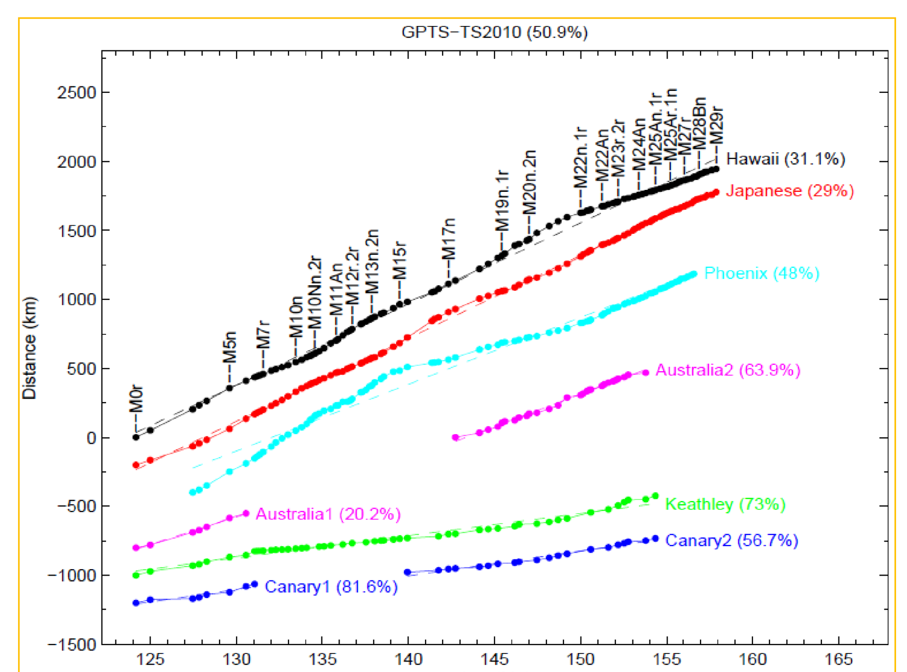

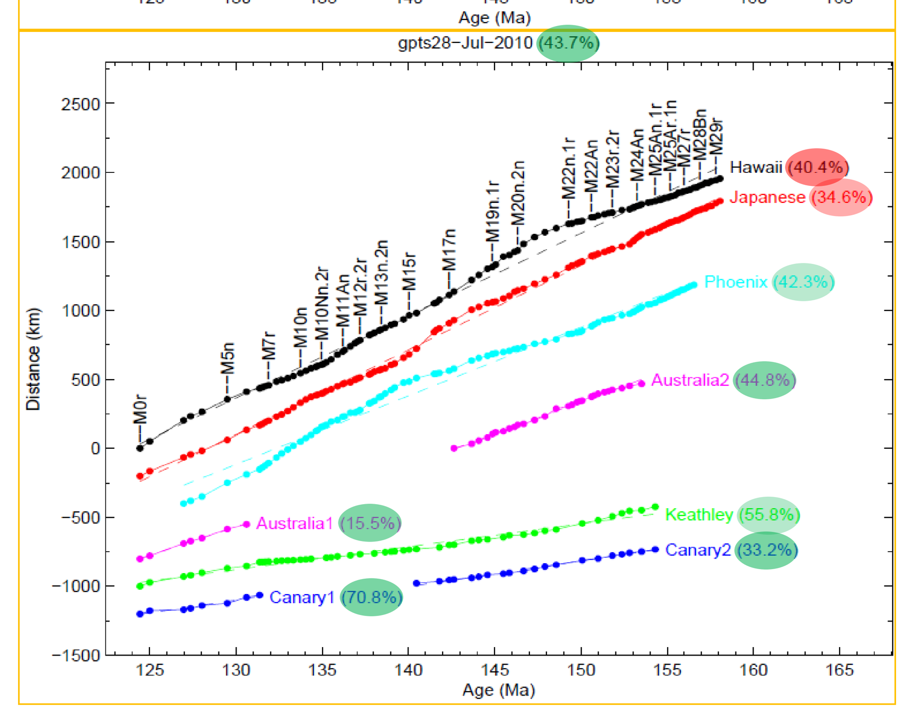

Fig. 11: (Right, top) Distance vs. time plot for the Tominaga and Sager timescale. Overall variance is marked in the title, and individual variances are displayed in the labels.
Fig. 12: (Right, bottom) Distance vs. time plot for a 1 million iteration run of the Metropolis loop. This is a bit of overkill, as there was no considerable difference between runs of even just 100 and 500 thousand iterations.

References

-Channell, et al. (1995). "Late Jurassic-early Cretaceous time scales and oceanic magnetic anomaly block models." *Geochronology, Time Scales, and Global Stratigraphic Correlation*, SEPM Special Publication No. 54, 51-63.
-Chib, S. and Greenberg, E. (Nov. 1995) "Understanding the Metropolis-Hastings Algorithm." The American Statistician, Vol. 49, No. 4, 327-335.
-Fiet, N. and Gorin, G. (2000). "Lithological expression of Milankovitch cyclicity in carbonate-dominated, pelagic, Barremian deposits in central Italy." *Cretaceous Research*, Vol. 21, 457-467.
-Gradstein, et al. (2005). "A Geological Time Scale 2004." Cambridge University Press, Cambridge.
-Malinverno, A., Erba, E., and Herbert, T.D. (2010). "Orbital tuning as an inverse problem: Chronology of the Early Aptian Oceanic Anoxic Event 1a (Selli Level) in the Cismon APTICORE." *Paleoceanography*, 25, PA2203, doi:10.1029/2009PA001769.
-Tominaga, M. and Sager, W. (2010). "Revised Pacific M-anomaly geomagnetic polarity timescale." *Geophysical Journal International*, 1-30, doi: 10.1111/j.1365-246X.2010.04619.x.